Validation of Proposed Analytical Model and Design Procedures for Multi-panel CLT Shearwalls Through Experimental Investigation

Mohammad Masroor, Ghasan Doudak, and Daniele Casagrande

Abstract Multi-panel CLT shearwalls are expected to provide more flexibility and energy dissipation than single-panel walls, mainly due to the contribution of the vertical joints between panels. Despite several analytical models and design approaches being proposed in the literature, timber design standards provide limited guidelines on the lateral and capacity-based design approaches for CLT shearwalls. This shortcoming is mainly due to inadequate experimental results on multi-panel CLT shearwalls to help validate the developed equations and substantiate the proposed kinematic modes and shearwall behaviour. This study investigates the lateral behaviour of CLT shearwalls by carrying out two full-scale testing on shearwalls consisting of three panels and subjected to monotonic lateral load. The experimental results were used to validate results obtained from proposed analytical expressions and numerical models. Connection-level monotonic tests were also carried out on hold-down and panel-to-panel joints to be used as the input for the analytical expressions and numerical models. Preliminary results from two shearwalls tests are presented in this paper, and comparisons to the numerical models show a reasonable match.

Keywords Structural capacity · Seismic risk · Mixes structural · Timber planks · Carrés de madriers · Finite element (FE) · ABAQUS

M. Masroor (✉) · G. Doudak
Department of Civil Engineering, University of Ottawa, Ottawa, Canada
e-mail: mmas100@uottawa.ca

D. Casagrande
Institute of Bioeconomy—National Research Council of Italy (CNR-IBE), Trento, Italy

1 Introduction

Cross-laminated timber (CLT) shearwalls have been increasingly used in timber constructions, primarily due to the high in-plane strength and stiffness of the CLT panels, as well as the wall's ability to dissipate energy through controlled failure mechanisms in the connections. These primarily include energy-dissipative joints between individual panels and capacity-protected connections between wall panels and supporting floors or foundations. These capabilities make CLT shearwalls a suitable alternative for mid- to high-rise buildings to those composed of steel and concrete.

CLT shearwalls can be composed of a single or multiple panels, which can have significant impact on their mechanical performance. When using commonly available joints, multi-panel CLT shearwalls are expected to provide more flexibility and energy dissipation, which is particularly suitable for high seismic regions. The majority of the energy dissipation is expected to be achieved in the joints attaching adjacent panels, since they typically consist of small diameter fasteners, such as nails or screws.

Several studies have been conducted with the aim to develop analytical models and design procedures for CLT multi-panel shearwalls. Gavric et al. [13] and Flatscher et al. [12] developed analytical expressions for single and two-panel walls and conducted experimental tests to validate the proposed models. Casagrande et al. [5] and Nolet et al. [16] developed analytical equations considering the elastic and elastic-perfectly plastic behaviour of the connections, assuming that only hold-down and panel-to-panel connections (i.e. vertical joints) contribute to the rocking behaviour, whereas angle brackets only behave in shear to prevent sliding. Masroor et al. [14] extended the applicability of the equations to include the bidirectional (i.e. combined uplift and shear) contribution of the angle brackets and hold-down.

Casagrande et al. [6] proposed a capacity-based design (CD) approach for light-frame and single- and multi-panel CLT shearwalls, based on the analytical expressions proposed by Casagrande et al. [5] and Nolet et al. [16]. It was reported that the seismic energy dissipation occurs primarily in panel-to-panel connections, whereas non-dissipative elements, such as CLT panels, were required to remain elastic. The proposal was extended by Masroor et al. [15] to also include the bidirectional contribution of the angle brackets. Casagrande et al. [4] summarized the developed CD approaches and proposed design provisions based on the Canadian and European wood design standards [7, 8].

Despite several analytical models and design approaches being proposed in the literature, timber design standards (e.g. [8]) only provide limited guidelines on the lateral capacity and stiffness of multi-panel CLT shearwalls. The lack of analytical and design expressions has resulted in designers lacking the needed resources and adequate knowledge to design such structures. This shortcoming might be attributed to inadequate experimental testing on multi-panel CLT shearwalls, especially with walls containing more than two panels, in order to validate the developed equations and substantiate the proposed kinematic behaviour. The research includes a comprehensive experimental study with the aim to develop a database of full-scale
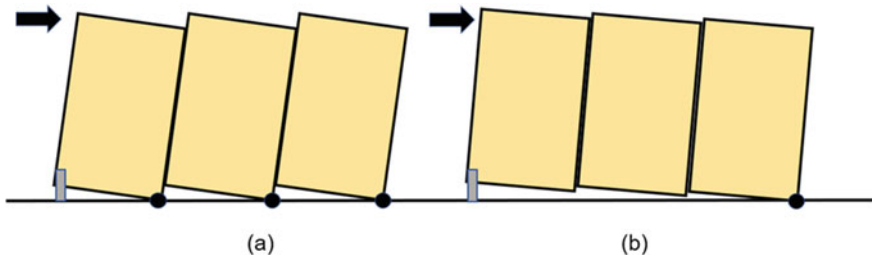
Fig. 1 **a** CP kinematic mode **b** SW kinematic mode

test results for CLT shearwalls undergoing various kinematic behaviours and failure modes. The paper provides updates on the ongoing testing programme and presents some preliminary results from the connection and full-scale testing campaign.

2   Objective

The current research has been established with the aim to carry out full-scale experimental tests on shearwalls containing three panels and subjected to monotonic lateral loading. The main goal of the current study is to validate the analytical expressions and numerical models available in the literature (e.g. [5, 16]). The study is limited in scope to shearwalls where the contribution of the angle brackets to the rocking behaviour is omitted. Two examples from the experimental campaign, related to the most common kinematic behaviour, namely coupled panel (CP) and single wall (SW) (Fig. 1), are presented and discussed. The results obtained from the analytical, numerical, and experimental tests are compared in terms of kinematic modes, displacements, and strength capacity. Connection-level monotonic tests were also carried out on hold-downs subjected to uplift and panel-to-panel connections subjected to shear loads, with the aim to be utilized as input in the analytical and numerical models.

3   Experimental Tests on Connections

The connection-level tests were conducted for hold-downs and panel–panel joints subjected to uplift and shear forces, respectively. Two repeat specimens were considered for each connection. The displacement rate used during the testing was 3 mm/min for the hold-down and 4.5 mm/min for the panel-to-panel connections, in order to achieve failure within 10 min. The WHT620 hold-down connection [10] consisted of a 3-mm-thick steel bracket with 55 (fully nailed) and 22 (partially nailed) LBA 4×60 mm threaded annular ring nails, 20-mm-thick washer, and 20-mm bolt, as

illustrated in Fig. 2a. The panel-to-panel connection was composed of HBS 6 × 70 mm screws, as shown in Fig. 2b [11].

Figure 3 presents the test set-up for the hold-down under monotonic uplift load. The CLT panel consisted of three layers, E1 grade, in accordance with ANSI/APA [1]. The total thickness of the panel was 105 mm (i.e. layer thickness of 35 mm), and the width of the individual boards was 89 mm.
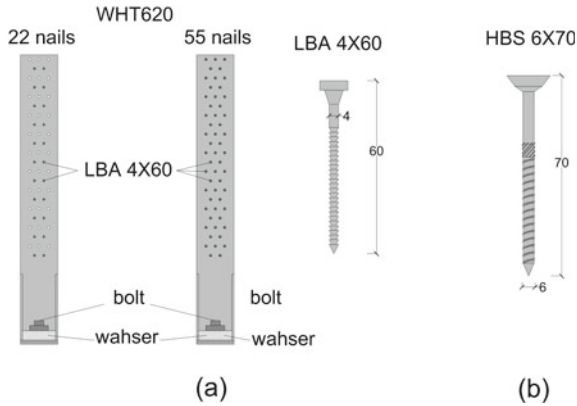

Fig. 2 **a** Hold-down connection WHT620. **b** Panel-to-panel screw connection HBS 6 × 60 mm
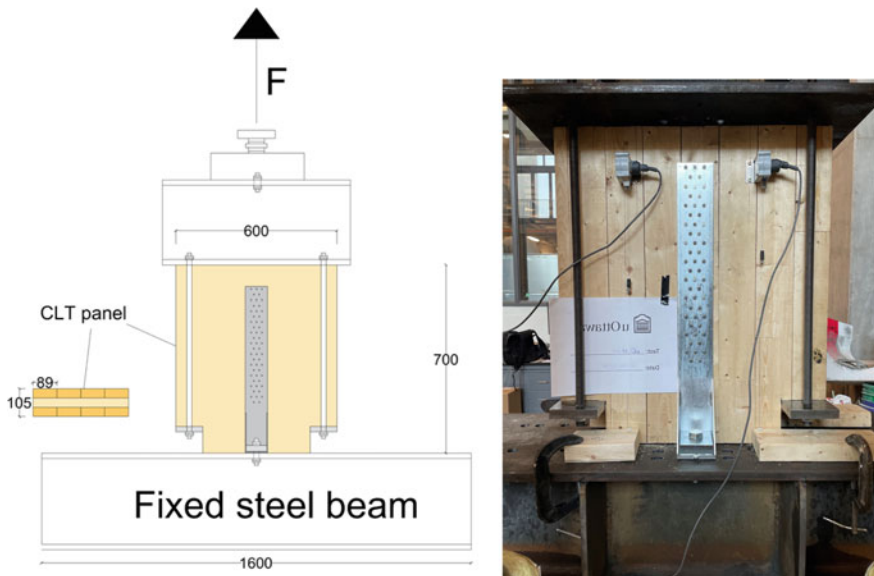

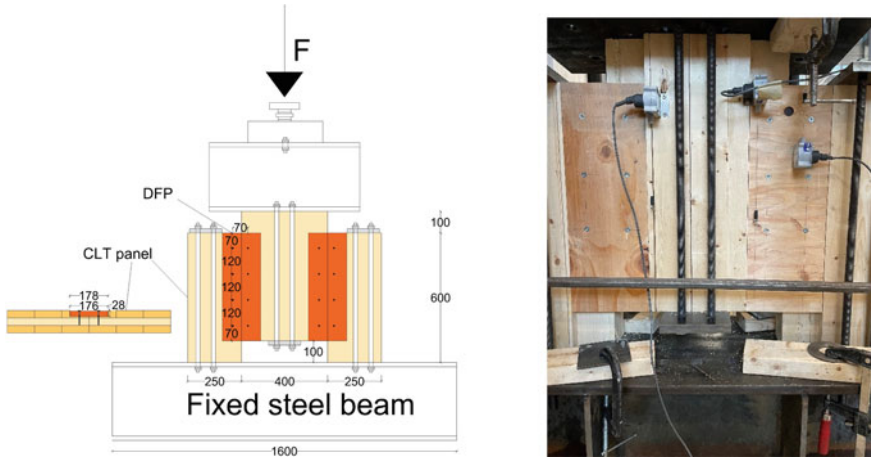**Fig. 3** Test set-up of hold-down connection

Fig. 4 Test set-up of panel-to-panel connection

The panel-to-panel connection specimen consisted of three CLT panels joined together with HBS 6 × 70 mm screws, as shown in Fig. 4. The connection represented a half-lap joint, using D-Fir plywood (DFP) with thickness of 25.5 mm and width of 176 mm. Fastener spacing of 120 mm was used to meet the minimum requirements in the CSA O86-19 [8] standard and to limit splitting in the wood.

Figure 5 presents the force–displacement curves for two repetitions for each of the fully nailed hold-down (HD-F-1 and HD-F-2), partially nailed hold-down (HD-P-1 and HD-P-2), and vertical joint (VJ-1 and VJ-2) tests. The graphs represent the behaviour of a single hold-down and a pair of panel-to-panel screw joint (i.e. two screws connecting the plywood side plate to two CLT wall panels). Table 1 summarizes the maximum applied loads from the tests, F_{max}, and its respective displacement, v_{max}, and presents the mechanical properties obtained from the curves using the equivalent energy elasto-plastic (EEEP) bilinear simulation, in accordance with ASTM E2126 [2]. This idealization of the connection behaviour is intended to be used in the analytical expressions. r_y and d_y are the yield strength and displacement, respectively, k represents the elastic stiffness, d_u is the ultimate displacement, and D_{EEEP} is for the ductility, obtained as the ratio between the ultimate and yield displacements.

The failure mechanisms observed from the experimental testing on hold-downs consisted of tensile tension failure in the vertical steel plate near the first row of nails for the fully nailed, as shown in Fig. 6a, and failure in the nails due to the cap breakage combined with nail withdrawal and bending for the partially nailed, as shown in Fig. 6b. The panel-to-panel connection failure was represented by a ductile failure mode, in which embedment crushing failure in the plywood and CLT combined with yielding in the fasteners was observed, as shown in Fig. 6c.
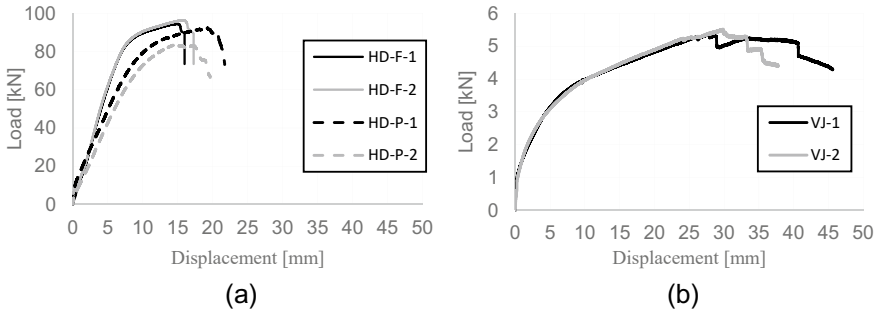
Fig. 5 Connections force–displacement curve for **a** hold-down and **b** panel-to-panel connection

Table 1 Mechanical properties of connections obtained from experimental tests

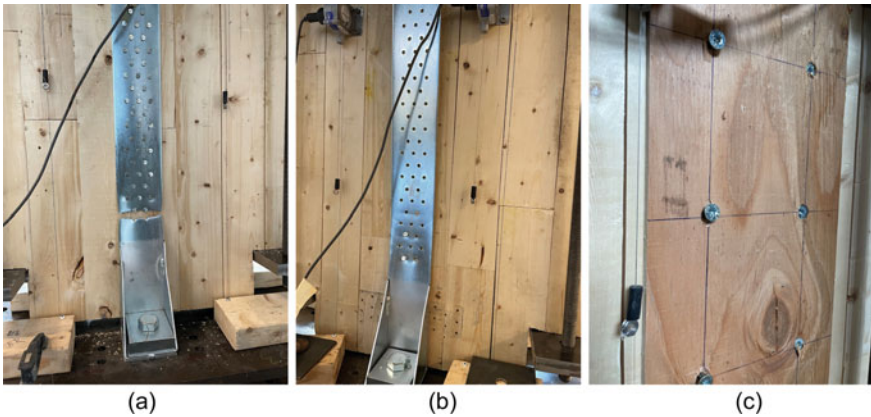| Connection	Test		EEEP simulation				
	F_{max} (kN)	v_{max} (mm)	r_y (mm)	d_y (mm)	k (kN/mm)	d_u (mm)	D_{EEEP} (–)
HD-F-1	94.5	14.9	89.8	7.43	12.1	16.0	2.15
HD-F-2	96.4	15.7	91.8	7.17	10.5	17.3	2.24
HD-P-1	92.31	19.29	85.82	9.16	9.36	21.71	2.37
HD-P-2	83.92	14.91	78.0	9.44	8.26	19.63	2.08
VJ-1	5.37	27.80	4.69	5.82	0.71	45.6	7.83
VJ-2	5.52	29.86	4.62	5.10	0.83	37.7	7.39

Fig. 6 Failure in: **a** fully nailed hold-down, **b** partially nailed hold-down, and **c** panel-to-panel joints

4   Investigation on Multi-panel CLT Shearwalls

Two CLT shearwalls with the configurations showed in Fig. 7 were investigated by conducting experimental tests. The height and total length of the shearwall were equal to 2438 mm and 3657 mm, respectively. Hold-down and panel-to-panel connections, consistent with those tested in the joint-level tests (i.e. WHT620 and HBS 6 × 70), were utilized to anchor the wall to the steel base. The same type of CLT panels that was used in the connection-level tests was also used in the full-scale shearwall tests. Table 2 presents the connection types and configurations and provides the anticipated kinematic modes. The number of panel-to-panel joints and the stiffness and yield strength of the hold-down and vertical joint connections were selected based on preliminary numerical runs to ensure that CP and SW behaviour are obtained in Test #1 and #2, respectively. No gravity load was considered in these tests; however, the weight of the panels and various test set-up attachments were estimated to be equal to 1.45 kN/m and considered in numerical and analytical models.
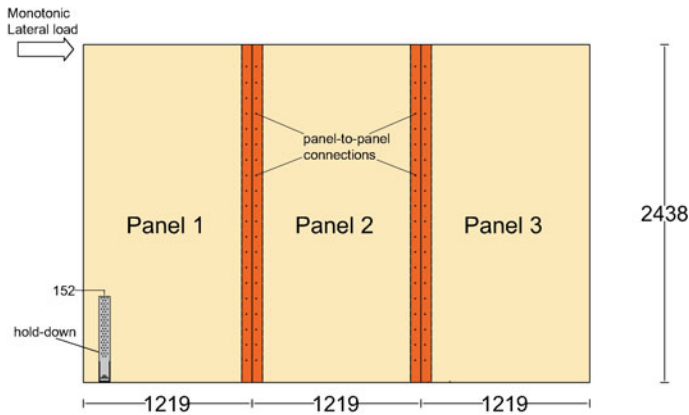

Fig. 7 Three panels CLT shearwall used for numerical and analytical models and experimental tests

Table 2 Number of connections and kinematic mode

Test	Number of hold-downs	Number of panel-to-panel connections	Nailing of the hold-down	Expected kinematic mode
#1	2	9	Fully nailed (55 nails)	CP
#2	1	35	Partially nailed (22 nails)	SW

4.1 Numerical and Analytical Investigations

Figure 8 presents the numerical model developed using the SAP2000 software [9]. The connections were modelled using multi-linear link elements representative of the real curves obtained from the connection tests. A concentrated lateral load is applied at the top of the wall, consistent with the loading actuator position in the experimental tests. A uniformly distributed gravity load, q, of 1.45 kN/m was applied on top of the wall to account for the weight of the panels and test set-up attachments. Sliding was prevented in the model by restraining horizontal movement at the centre of rotation of each panel, and gap elements, which are only active in compression, were assigned a high stiffness equal to 10^8 MPa to simulate the contact between the panels and the base. Diaphragm constraints were considered at the top and bottom of the panels.

The CLT panels were modelled with orthotropic material properties. The values of E_0, E_{90}, and G_0 were obtained from Canadian wood design standard [8] for E1 CLT grade and were equal to 11,700, 300, and 731 MPa, respectively. The effective moduli, utilized to define the orthotropic material properties, $E_{\text{eff},1}$ (along the horizontal direction) $E_{\text{eff},2}$ (along the vertical direction), and G_{eff}, are obtained using Eqs. 1–4, based on work by Brandner et al. [3].

$$E_{\text{eff},1} = \frac{E_0 \cdot t_{90} + E_{90} \cdot t_0}{t_{\text{CLT}}} = \frac{11700 \cdot 35 + 300 \cdot 70}{105} = 4100\,\text{MPa} \qquad (1)$$

$$E_{\text{eff},2} = \frac{E_0 \cdot t_0 + E_{90} \cdot t_{90}}{t_{\text{CLT}}} = \frac{11700 \cdot 70 + 300 \cdot 35}{105} = 7900\,\text{MPa} \qquad (2)$$

$$\alpha = 0.53 \cdot \left(\frac{t_{\text{mean}}}{w}\right)^{-0.79} = 0.53 \cdot \left(\frac{35}{89}\right)^{-0.79} = 1.11 \qquad (3)$$
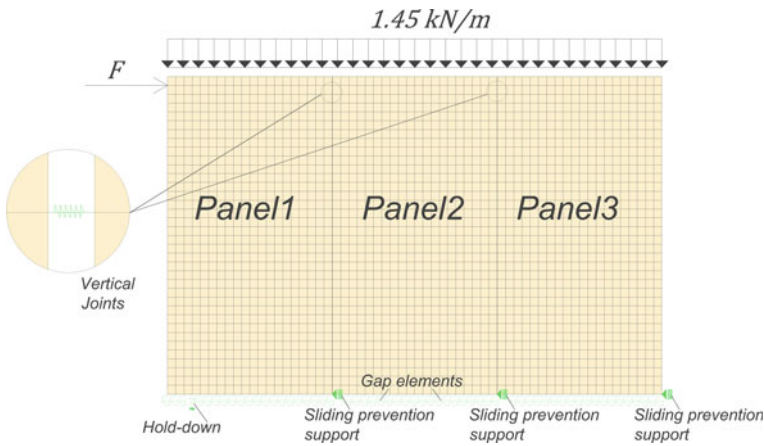

Fig. 8 Numerical model of a three-panel CLT shearwall in SAP2000

$$G_{\text{eff}} = \frac{G_0}{1 + 6 \cdot \alpha \cdot \left(\frac{t_{\text{mean}}}{w}\right)^2} = \frac{731}{1 + 6 \cdot 1.11 \cdot \left(\frac{35}{89}\right)^2} = 361.1\,\text{MPa}, \qquad (4)$$

where t_0 and t_{90} are the total thicknesses of the longitudinal (vertical) and transverse (horizontal) layers, t_{CLT} is the total thickness of the panel, and w is the width of laminations.

Nolet et al. [16] presented analytical procedures to obtain the rocking behaviour of three-panel CLT shearwalls for CP and SW kinematic modes, as illustrated in Fig. 9. Table 3 summarizes the expressions required in the analytical procedures and the respective values defining the shearwall behaviour from Fig. 9. The expressions for CP were updated by factors γ_1 and γ_2 to account for the real position of the hold-down and the loading actuator in experimental tests. These variables represent the ratio of the distance between the centre of rotation of the first panel and the hold-down to the length of each panel (b) and the ratio of the distance between the bottom of the wall and the position of the lateral load to the height of the wall. The analytical equations are calculated using the mechanical properties for connections obtained from the EEEP curves (Table 1) for hold-down and vertical joints. Additional subscripts associated with each connection are included in each parameter, such as h for the hold-down and c for panel-to-panel connection. As such, n_c represents the number of joints between adjacent panels.

Table 3 Analytical expressions developed by Nolet et al. [16] and their respective values

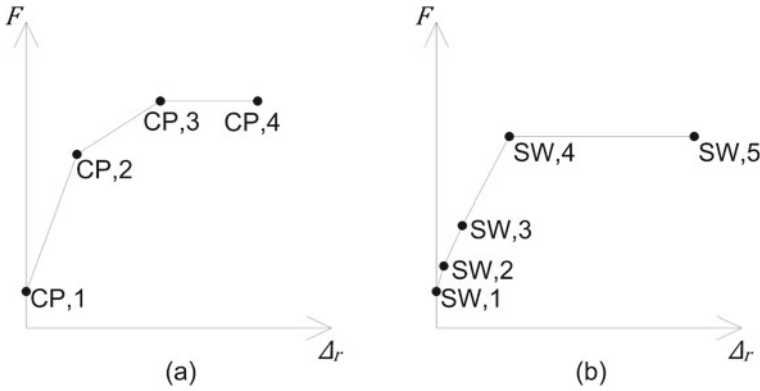| Point	Expression		Values	
	F	Δ_r	F (kN)	Δ_r (mm)
CP,1	$\frac{q \cdot m \cdot b^2}{2 \cdot h \cdot \gamma_2}$	–	1.32	0
CP,2	$\frac{[\gamma_1^2 \cdot k_h + (m-1) \cdot n_c \cdot k_c] b}{k_c \cdot \gamma_2} + \frac{q \cdot m \cdot b^2}{2 \cdot h \cdot \gamma_2}$	$d_{y,c} \cdot \frac{h}{b}$	90.84	9.34
CP,3	$\frac{b}{h \cdot \gamma_2} \cdot \left[\gamma_1 \cdot r_h + r_c \cdot (m-1) \cdot n_c + \frac{q \cdot m \cdot b}{2} \right]$	$\frac{d_{y,h}}{\gamma_1} \cdot \frac{h}{b}$	134.32	17.74
CP,4	$\frac{b}{h \cdot \gamma_2} \cdot \left[\gamma_1 \cdot r_h + r_c \cdot (m-1) \cdot n_c + \frac{q \cdot m \cdot b}{2} \right]$	$\min\left(d_{u,c}, \frac{d_{u,h}}{\gamma_1}\right) \cdot \frac{h}{b}$	134.32	39.72
SW,1	$\frac{q \cdot m \cdot b^2}{2 \cdot h}$	–	1.32	0
SW,2	Equation (5)	Equation (6)	3.93	0.14
SW,3	Equation (7)	Equation (8)	6.50	0.30
SW,4	$\frac{1}{h} \cdot \left[r_h \cdot m \cdot b + \frac{q \cdot m^2 \cdot b^2}{2} \right]$	Equation (9)	120.98	9.25
SW,5	$\frac{1}{h} \cdot \left[r_h \cdot m \cdot b + \frac{q \cdot m^2 \cdot b^2}{2} \right]$	$\Delta_{r,\text{SW},4} + \left[\frac{h}{m \cdot b} \cdot \left(d_{u,h} - d_{y,h} \right) \right]$	120.98	15.97

Fig. 9 Analytical curves developed by Nolet et al. [16]: **a** for CP; **b** for SW

$$F_{\text{SW},2} = \frac{q \cdot m^2 \cdot b^2}{2 \cdot h} \cdot \frac{k_h \cdot \left(\frac{3 \cdot m - 2}{m^2}\right) + \left(\frac{2 - m}{m^2}\right)}{n_c \cdot k_c - k_h} \tag{5}$$

$$\Delta_{r,\text{SW},2} = \left(F_{\text{SW},2} - \frac{q \cdot m \cdot b^2}{2 \cdot h}\right) \frac{h^2}{b^2 \cdot [k_h + (m-1) \cdot n_c \cdot k_c]} \tag{6}$$

$$F_{\text{SW},3} = \frac{q \cdot m^2 \cdot b^2}{2 \cdot h} \cdot \frac{k_h \cdot \left(\frac{m+6}{m^2}\right) + \left(\frac{5 \cdot m - 6}{m^2}\right)}{n_c \cdot k_c - k_h} \tag{7}$$

$$\Delta_{r,\text{SW},3} = \left(F_{\text{SW},3} - \frac{q \cdot m \cdot b^2}{2 \cdot h}\right) \frac{h^2 \cdot [k_h + n_c \cdot k_c]}{b^2 \cdot [(m+2) \cdot k_h + (m-2) \cdot n_c \cdot k_c] \cdot n_c \cdot k_c} \tag{8}$$

$$\Delta_{r,\text{SW},4} = \left\{ \frac{F_{\text{SW},4} \cdot h^2}{b^2} - \left[\frac{\left(\frac{1}{k_h} + \frac{m-1}{n_c \cdot k_c}\right)^{-1}}{k_h} \cdot \frac{q \cdot m^2}{2 \cdot h} \right] \right\} \cdot \frac{1}{m^2 \cdot \left(\frac{1}{k_h} + \frac{m-1}{n_c \cdot k_c}\right)^{-1}}, \tag{9}$$

where $F_{\text{SW},i}$ is the lateral load at point SW, i for $i = 2{:}4$.

Since the analytical expressions were developed assuming rigid behaviour of the CLT panels, bending and shear deformations of panels are added to account for the flexibility in the panels. These are calculated using Eqs. (10) and (11) for bending and shear deformations, respectively.

$$\Delta_b = \frac{F \cdot h^3}{3 \cdot \text{EI}_{\text{eff}}} \tag{10}$$

$$\Delta_{\text{sh}} = \frac{F \cdot h}{G_{\text{eff}} \cdot t_{\text{CLT}} \cdot m \cdot b}, \tag{11}$$

where F is the lateral load and G_{eff} is obtained from Eq. (4).

The value for EI_{eff} for CP and SW can be calculated using Eqs. (12) and (13), respectively.

$$EI_{eff,CP} = m \cdot \left(E_0 \cdot t_0 \cdot \frac{b^3}{12} + E_{90} \cdot t_{90} \cdot \frac{b^3}{12} \right) = 3.76 \times 10^{14} \, \text{N mm}^2 \qquad (12)$$

$$EI_{eff,SW} = E_0 \cdot t_0 \cdot \frac{(b \cdot m)^3}{12} + E_{90} \cdot t_{90} \cdot \frac{(b \cdot m)^3}{12} = 3.38 \times 10^{15} \, \text{N mm}^2. \qquad (13)$$

4.2 Experimental Tests on Shearwalls

The experimental test configuration is illustrated in Fig. 10. Horizontal support mechanisms were designed and implemented at the base of each panel in order to prevent sliding, while allowing free rotation. In an actual CLT wall, construction sliding would be limited by angle brackets, which as mentioned earlier would contribute to the shear and uplift of the wall panels. Future testing will investigate the effect of angle brackets on the shearwall behaviour. The displacement rate at the top of the walls was selected to 6 mm/min in order to achieve consistent displacement rates between the connection-level and full-scale level tests.

Figure 11 presents the force–displacement curves obtained from the two tests. Comparisons between the two curves show that more ductility can be observed in test #1 since the wall behaviour is dominated by the engagement of the panel-to-panel connections. Wall test #2 exhibited higher stiffness but significantly lower ductility due to rigid connections between the panels, resulting in the wall behaving almost like a single-panel wall. The ductility of the wall is primarily driven by the behaviour of the hold-down connection which is less ductile than the panel-to-panel joints (refer to Fig. 5).

Figures 12 and 13 present the failure mechanism obtained at the end of test #1 and #2, respectively, and highlight that the failure in the connections at the shearwall level was consistent with those obtained at the connection-level tests. It is important to note that the walls achieved the anticipated kinematic modes, as indicated in Table 2, where wall test #1 exhibited CP kinematic mode while wall test #2 attained SW kinematic mode, as shown in Figs. 12 and 13, respectively. Table 4 summarizes the results obtained from the tests and includes the parameters obtained from the idealized EEEP curve.
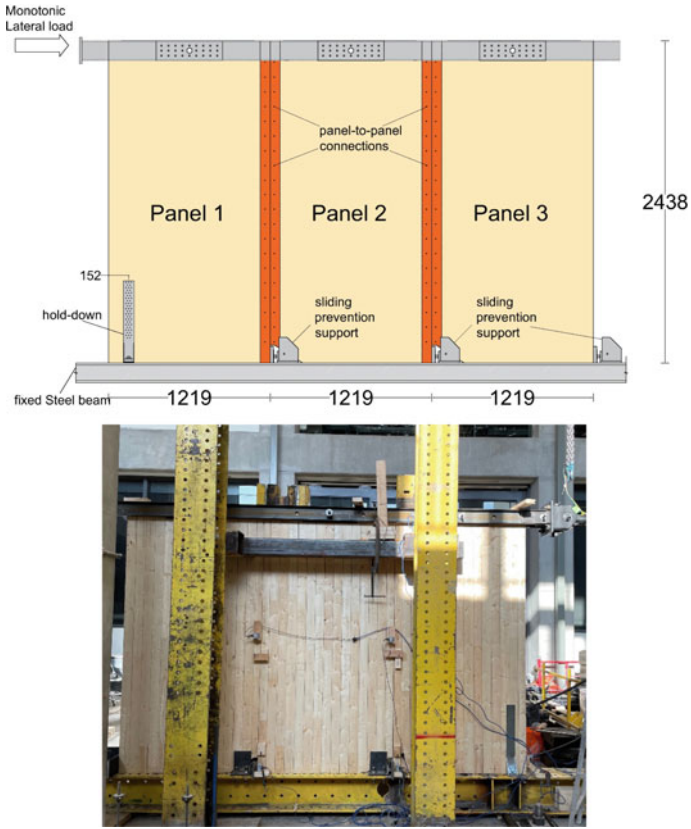
Fig. 10 Set-up of CLT shearwall test

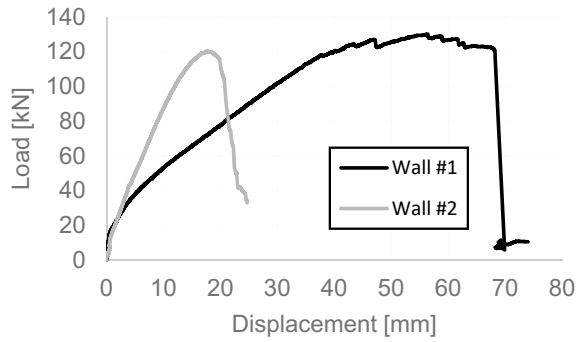**Fig. 11** Force–displacement curve for shearwalls experimental tests

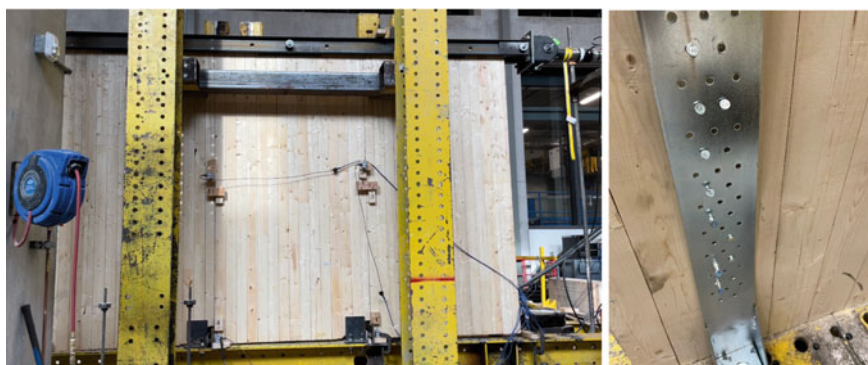**Fig. 12** Lateral behaviour and failure of CLT shearwall experimental test #1

Fig. 13 Lateral behaviour and failure of CLT shearwall experimental test #2

Table 4 Results of experimental tests on CLT shearwalls

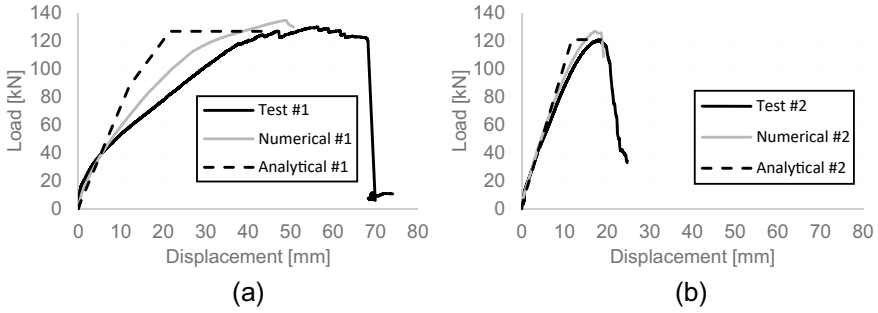| Test	F_{max}(kN)	v_{max}(mm)	$F_{y,EEEP}$(mm)	$v_{y,EEEP}$(mm)	k_{EEEP}(kN/mm)	$v_{u,EEEP}$(mm)	D_{EEEP}(−)
#1	130.0	56.39	114.96	24.55	4.68	68.2	2.78
#2	120.3	17.70	109.49	11.76	9.31	20.84	1.77

Fig. 14 Experimental, numerical, and analytical curves of the shearwalls: **a** wall #1; **b** wall #2

4.3 Discussion

Figure 14 presents the three curves obtained from the experimental results, numerical and analytical models for wall #1 and wall #2. As can be observed, reasonable match can be found in terms of the general behaviour and the shape of the curves for both walls. In particular, the match between the models and test results for the wall dominated by SW behaviour is close due to the fact that the behaviour is generally dominated by the hold-down mechanical properties. Wall #1 involves a more complex behaviour where both the hold-down and the vertical joints participate in the performance of the wall.

Table 5 summarizes the key parameters obtained from each method, including the percentage difference between experimental test and numerical model results, denoted as $\xi_{T/N}$, and between experimental test and analytical model results, denoted as $\xi_{T/A}$. The results show that the maximum force, F_{max}, and yield force, $F_{y,EEEP}$ match reasonably well with maximum difference of 6% and 10%, respectively. Maximum displacement, v_{max}, and yield displacement, $v_{y,EEEP}$, present more deviation between the results for wall #1, with difference around 18% for the numerical model and 14% for analytical model, whereas for wall #2 the maximum difference was 8%. For the elastic stiffness, k_{EEEP}, and ultimate displacement, $v_{u,EEEP}$, significant differences were observed especially for wall #1, with 21% and 35% for the numerical model and 54% and 63% for the analytical model, respectively. The stiffness is notoriously difficult to estimate due to the nonlinear nature of the behaviour of wood shearwalls even at low displacement levels. The ultimate displacement is also particularly difficult to predict since the behaviour of post yield and peak loads is erratic and depends on multiple failure mechanisms. The significant discrepancy observed in the analytical model, especially for wall #1, could be attributed to using the EEEP idealization curve for the panel-to-panel connections. It can be observed that significantly better fit is obtained for wall #1 in numerical model owing to using the real connection curve obtained from the joint-level tests.

Table 5 Results obtained from experimental tests and numerical and analytical models

Wall	Content	F_{max}(kN)	v_{max}(mm)	$F_{y,EEEP}$(mm)	$v_{y,EEEP}$(mm)	k_{EEEP}(kN/mm)	$v_{u,EEEP}$(mm)	D_{EEEP}(−)
#1	Test	130.07	56.39	114.96	24.55	4.68	68.21	2.78
	Numerical	134.64	48.98	117.59	20.75	5.68	50.62	2.44
	Analytical	126.93	–	126.93	21.49	7.23	41.91	1.69
	$\xi_{T/N}$	4%	15%	2%	18%	21%	35%	14%
	$\xi_{T/A}$	2%	–	10%	14%	54%	63%	64%
#2	Test	120.25	17.70	109.49	11.76	9.31	20.84	1.77
	Numerical	126.98	17.18	114.21	10.91	10.47	19.14	1.75
	Analytical	120.98	–	120.98	11.73	10.13	18.51	1.58
	$\xi_{T/N}$	6%	3%	4%	8%	12%	9%	1%
	$\xi_{T/A}$	1%	–	10%	0%	9%	13%	12%

5 Conclusion

The lateral behaviour of CLT shearwalls was studied by carrying out two wall-level experimental tests on three-panel walls under monotonic lateral load. The results were compared with numerical and analytical models. The key findings of this research can be summarized as follows:

- The connection-level tests showed that the failure mechanisms observed in the hold-downs were of tension failure in the vertical steel plate near the first row of nails for the fully nailed, while failure in partially nailed hold-downs was in cap breakage combined with nail withdrawal and bending. The panel-to-panel connections were represented by a ductile failure mode, in which embedment crushing failure in the plywood and CLT combined with yielding in the fasteners was observed.
- Two experimental tests on CLT shearwalls were carried out, using the same type of CLT panels and connections used in the joint-level tests. Force–displacement curves and respective properties of each wall were presented. The wall with SW behaviour exhibited higher stiffness but significantly lower ductility due to the rigid connections between adjacent panels.
- Numerical and analytical models were evaluated, and results were compared with those obtained through the experimental tests. Reasonable match was observed in terms of the general behaviour and the shape of the curves in both walls. The values for maximum and yield forces showed reasonable match for both walls, while differences were found in the elastic stiffness and ultimate displacement, especially for the wall that exhibited CP behaviour.

References

1. ANSI/APA (2020) ANSI/APA PRG 320:2019 standard for performance-rated cross-laminated timber. APA—The Engineered Wood Association
2. ASTM E2126 (2019) Standard test methods for cyclic (reversed) load test for shear resistance of vertical elements of the lateral force resisting systems for buildings
3. Brandner R, Dietsch P, Dröscher J, Schulte-Wrede M, Kreuzinger H, Sieder M (2017) Cross laminated timber (CLT) diaphragms under shear: test configuration, properties and design. Constr Build Mater 147:312–327. https://doi.org/10.1016/j.conbuildmat.2017.04.153
4. Casagrande D, Doudak G, Masroor M (2021) A proposal for capacity-based design of multi-storey CLT buildings. In: INTER—international network on timber engineering research
5. Casagrande D, Doudak G, Mauro L, Polastri A (2018) analytical approach to establishing the elastic behavior of multipanel CLT shear walls subjected to lateral loads. J Struct Eng 144(2):04017193. https://doi.org/10.1061/(ASCE)ST.1943-541X.0001948

6. Casagrande D, Doudak G, Polastri A (2019) A proposal for the capacity-design at wall- and building-level in light-frame and cross-laminated timber buildings. Bull Earthq Eng 17(6):3139–3167. https://doi.org/10.1007/s10518-019-00578-4
7. CEN (2004) European Standard EN 1995: Eurocode 5: Design of timber structures. European Committee for Standardization
8. CSA O86-19 (2019) Engineering design in wood. CSAO86:19. CSA Group
9. CSI (2018) SAP2000 integrated software for structural analysis and design (No. 18). Computers and Structures Inc.
10. European Technical Approval ETA-11/0086 (2018) European Organization for Technical approval
11. European Technical Assessment ETA-11/0030 (2019) European Organization for Technical approval.
12. Flatscher G, Bratulic K, Schickhofer G (2015) Experimental tests on cross-laminated timber joints and walls. Proc Inst Civ Eng Struct Build 168(11):868–877. https://doi.org/10.1680/stbu.13.00085
13. Gavric I, Fragiacomo M, Ceccotti A (2015) Cyclic behavior of CLT wall systems: experimental tests and analytical prediction models. J Struct Eng 141(11):04015034. https://doi.org/10.1061/(ASCE)ST.1943-541X.0001246
14. Masroor M, Doudak G, Casagrande D (2020) The effect of bi-axial behaviour of mechanical anchors on the lateral response of multi-panel CLT shearwalls. Eng Struct 224. https://doi.org/10.1016/j.engstruct.2020.111202
15. Masroor M, Doudak G, Casagrande D (2022) Design of multipanel CLT shear walls with bidirectional mechanical anchors following capacity-based design principle. J Perform Constr Fac 36(1). https://doi.org/10.1061/(ASCE)CF.1943-5509.0001693
16. Nolet V, Casagrande D, Doudak G (2019) Multipanel CLT shearwalls: an analytical method- ology to predict the elastic-plastic behaviour. Eng Struct 179:640–654. https://doi.org/10.1016/j.engstruct.2018.11.017